

# GAS FLOW IN NANO-CHANNELS: THERMAL TRANSPIRATION MODELS WITH APPLICATION TO A SI-MICROMACHINED KNUDSEN PUMP

Naveen K. Gupta<sup>1</sup>, Nathan D. Masters<sup>2</sup>, Wenjing Ye<sup>2</sup>, and Yogesh B. Gianchandani<sup>1</sup>

<sup>1</sup>Department of Mechanical Engineering, University of Michigan, Ann Arbor, MI-48109, USA.

<sup>2</sup>Department of Mechanical Engineering, Georgia Institute of Technology, Atlanta, GA-30332, USA.

**Abstract:** This paper presents a comparative study of performance of various analytical and semi-analytical models used for the analysis of rarefied gas flow, which is responsible for the phenomenon of thermal transpiration. In particular, these are evaluated in the context of the scaling analysis of a Si-micromachined monolithic Knudsen pump. Results from these models are verified using available experimental data and are benchmarked against the simulation results from direct simulation Monte Carlo (DSMC) technique. Characterization of Sharipov's model against the DSMC technique with the help of specially designed test cases predicts that Sharipov's model is potentially the most representative model for DSMC in this context. Finally, Sharipov's model is used to evaluate the sensitivity analysis of structural and performance parameters relevant for thermal transpiration. The analysis shows that for a 200  $\mu\text{m}$  long channel on a well-insulated glass substrate, with a channel height of 100 nm and 10  $\mu\text{m}$  width, provides a mass flow rate of  $1.5 \times 10^{-6}$  sccm with a  $\Delta T$  of 300  $^{\circ}\text{C}$ .

**Keywords:** Thermal transpiration, Knudsen pump, Monte Carlo, DSMC, Rarefied gas dynamics.

## I. INTRODUCTION

Thermal transpiration is characterized by an equilibrium pressure gradient generated along a narrow channel due to a temperature gradient along the channel [1, 2]. From the point of view of molecular dynamics, thermal transpiration can be explained as the equilibrium state attained by two opposing flow fields, thermal creep flow and Poiseuille flow (Fig. 1). The thermal creep flow is the movement of molecules near the walls from the cold end to the hot end. The counter flow, known as the Poiseuille flow, is induced by the pressure gradient generated by the thermal creep flow and it acts to nullify the same [3]. Flow at these scales is similar to rarefied gas flows encountered at macro scales. For example, gas in a channel with height 100 nm or less, will be rarefied even at atmospheric pressures.

The phenomenon of thermal transpiration has been known since the 1870s, and various researchers have contributed intermittently towards its understanding since then. One of most remarkable contribution is a thermal transpiration based vacuum pump that was proposed by Knudsen in 1910 [4]. Other microfluidic device like gas chromatographs and filters can also be affected by thermal transpiration [5].

The study presented here aims at identifying an alternative to molecular based numerical techniques such as direct simulation Monte Carlo (DSMC), which is an attractive tool for precise analysis of the phenomenon of thermal transpiration, but is computationally expensive [6, 7]. The DSMC results are validated against the available experimental data from a silicon micromachined Knudsen pump [8]. Subsequently, these DSMC results are used to benchmark results from various analytical models under consideration, and use the best model to perform

sensitivity analysis of various design parameters required for effective operation of a Knudsen pump.

## II. THEORETICAL MODELS

Figure 2 shows the computational flow of the DSMC technique, which has been established as a favored tool for flow through nanochannels. It tracks a statistically representative set of particles to predict the behavior of a system and can be understood as a sequence of the four basic steps: particle movement, particle indexing and cross referencing, collision simulation and sampling. The information available for particles at microscopic level is used to evaluate the macroscopic attributes of the system.

The analytical and semi-analytical models, such as those given by Maxwell [2], Knudsen [3], Kennard [9], Williams [10] and Sharipov [11] (Table 1A and 1B), are special cases of the Boltzmann equation (BE):

$$\frac{\partial f}{\partial t} + \bar{v} \cdot \frac{\partial f}{\partial \bar{x}} + \bar{F} \cdot \frac{\partial f}{\partial \bar{v}} = Q(f, f_*) \quad (1)$$

where,  $\bar{F}$  is imposed body force,  $\bar{v}$  is the velocity vector,  $\bar{x}$  position vector,  $f$  is the velocity density function, The time change in the density function ( $\partial f / \partial t$ ) is caused by the changes in  $f$  due to molecular motion ( $\bar{v} \cdot (\partial f / \partial \bar{x})$ ), external body force ( $\bar{F} \cdot (\partial f / \partial \bar{v})$ ) and collisions between molecules ( $Q(f, f_*)$ ).

In order to solve BE analytically, most of the models

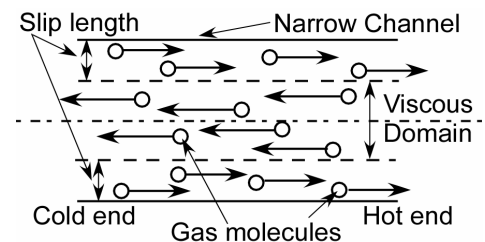


Fig. 1: Thermal Transpiration at molecular level.

for thermal transpiration use linearized BE with a simplified collision model, which becomes the primary constraint for applicability. The models by Kennard, Maxwell, and Williams assume a tube cross-section and are limited to slip flow, i.e.,  $Kn < 0.1$ . The Knudsen model has been empirically corrected for various  $Kn$ , but it also assumes circular cross-sections. Sharipov's model is for rectangular cross-sections, and uses the S-model to evaluate collisions between the molecules. It is valid for the entire flow regime, ranging from free-molecule flow to continuum flow.

### III. SIMULATION MODEL

These various models are applied to a device that was first described in [8] (Fig. 3 and 4). It has multiple narrow channels connecting two cavities (cavity 1 and cavity 2). The heated cavity (cavity 1) is further connected through a wide channel to cavity 3, which remains at ambient pressure and temperature. These large cavities ( $160 \times 50 \times 10 \mu\text{m}^3$ ) and the wide channel (X-section:  $30 \times 10 \mu\text{m}^2$ ), countersunk in a glass substrate, are capped by a  $\text{SiO}_2/\text{Si}_3\text{N}_4/\text{SiO}_2$  stack. The narrow channels (X-section:  $10 \times 0.1 \mu\text{m}^2$ ) have an additional micron-thick cap layer of polysilicon. A polysilicon heater present in hot cavity is fabricated so as to isolate it from the polysilicon layer used to define the narrow channels. This device achieves  $\approx 0.46 \text{ atm}$ .

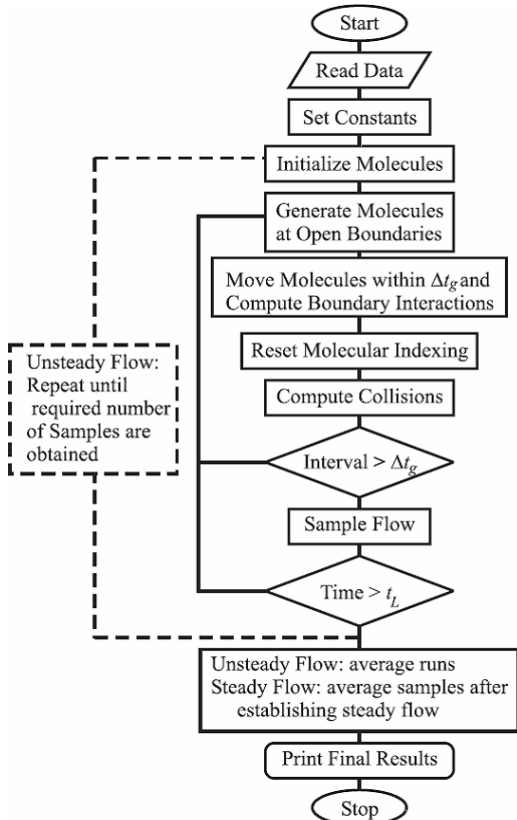


Fig. 2: The computational flow for DSMC technique

with 80 mW input power, with an estimated heater temperature of  $\approx 1373 \text{ K}$ .

ANSYS is used to compute the temperature distribution along the channel (Fig. 5), which serves as an input to various analytical models under consideration [12]. The ANSYS model assumes a fixed temperature boundary condition (300 K) at the base. A convection boundary condition is imposed on the top and side faces of the device with ambient at 300 K.

### IV. RESULTS AND DISCUSSION

Figure 6 shows the performance of each of these models relative to the DSMC simulation results. The results predicted by Kennard's, Williams' and Maxwell's models deviate significantly from the DSMC results, potentially because these models are valid only in the slip flow regime. Pressure distributions, as predicted by Sharipov's and Knudsen's models, closely match the DSMC results. Although, the Knudsen model is an empirically corrected model, yet assumes circular cross-sections. Hence, Sharipov's model emerges as the most promising semi-analytical model for thermal transpiration in this application context [9]. Further, the plots also indicate that for the system under consideration channel length can be reduced to  $200 \mu\text{m}$  without severely compromising the differential pressure achievable.

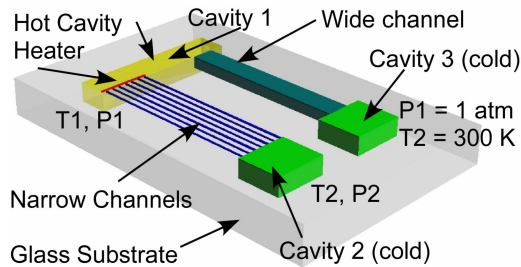


Fig. 3: Schematic layout of a single stage Knudsen pump.

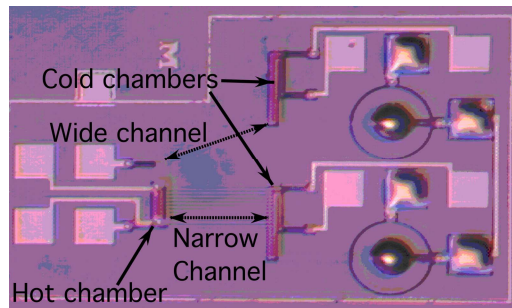


Fig. 4: Photograph of a single stage Knudsen pump used for experimental verification [8]

Sharipov's model numerically evaluates temperature and pressure flow coefficients for different flow regimes and over a wide range of height-to-width ratio of rectangular channels. Figure 7 compares an estimate of theoretical and experimental pressure difference at the ends of a  $700 \mu\text{m}$  long channel as a function of temperature at the hot end. The temperature profile for this case is extrapolated by scaling up/down the profile shown in Fig. 5, keeping the cold end temperature at 300 K. The mismatch between

Table 1A: (Semi) Analytical Models

Maxwell [2]:  $\frac{dp}{dT} = 6 \frac{\mu^2}{\rho T} \frac{1}{a^2 + 4Ga}$

Knudsen [3]:  $\frac{dp}{dT} = \frac{1}{\frac{8}{3} \frac{1}{k_1} \frac{a}{\lambda} + \frac{\pi}{16} \left(\frac{0.81}{0.49}\right) \frac{a^2}{\lambda^2} \frac{1}{k_1}} \frac{p}{2T}$

Kennard [9]:  $\frac{dp}{dx} = \frac{6\mu^2 R}{a^2 p \left(1 + \frac{4\zeta}{a}\right)} \frac{dT}{dx}$

Williams [10]:  $\frac{dp}{dx} = \frac{6\mu^2 R}{a^2} \left[ p + \frac{4\mu}{a} \left(\frac{2-\sigma}{\sigma}\right) \left(\frac{\pi RT}{2}\right)^{\frac{1}{2}} \right]^{-1} \frac{dT}{dx}$

Sharipov [11]:  $\frac{dp}{dx} = \frac{Q_T}{Q_P} \frac{P}{T} \frac{dT}{dx}$

Table 1B: Nomenclature

- P, T: Press. & temp. along the narrow channel
- P<sub>1</sub>, T<sub>1</sub>: Press. & temp. at hot end
- P<sub>2</sub>, T<sub>2</sub>: Press. & temp. at cold end.
- Viscosity,  $\mu = \left(\frac{1}{2}\right) Nm\bar{u}\lambda$
- Avg. vel.  $\bar{u} = \left(\frac{8RT}{\pi}\right)^{\frac{1}{2}}$
- Mean free path,  $\lambda = \frac{k_B T}{\sqrt{2}\pi D^2 P}$
- Knudsen #  $Kn = \frac{\lambda}{a}$
- # molecules/Vol  $N = \frac{P}{k_B T}$
- R<sub>g</sub>: Universal gas const
- ζ: Slip length
- σ: Mol reflection coeff.
- k<sub>B</sub>: Boltzmann constant
- Gas constant, R = R<sub>g</sub>/M
- N<sub>A</sub>: Avagadro Number
- Density, ρ = Nm
- M: Mol. mass of gas
- D: Collision diameter
- Mass of a single molecule m = M/N<sub>A</sub>.
- a: hydraulic radius
- k<sub>1</sub>=1 if Kn>>1, else 2<k<sub>1</sub><3
- G (= 2λ) is coefficient of slipping

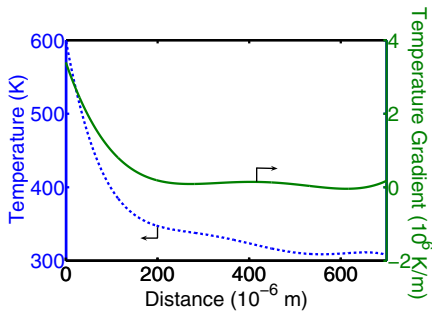


Fig. 5: The local temperature and its gradient along the channel for a single stage pump (ANSYS).

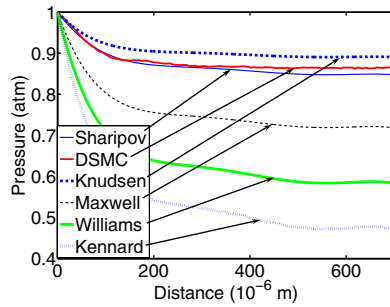


Fig. 6: Pressure distribution along the channel, as predicted by various models using temperature profile from Fig. 5.

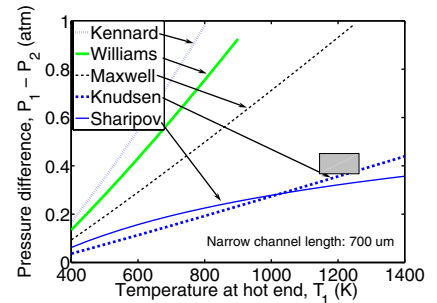


Fig. 7: Total pressure drop for the narrow channel as function of T<sub>1</sub>. The box shows experimental data.

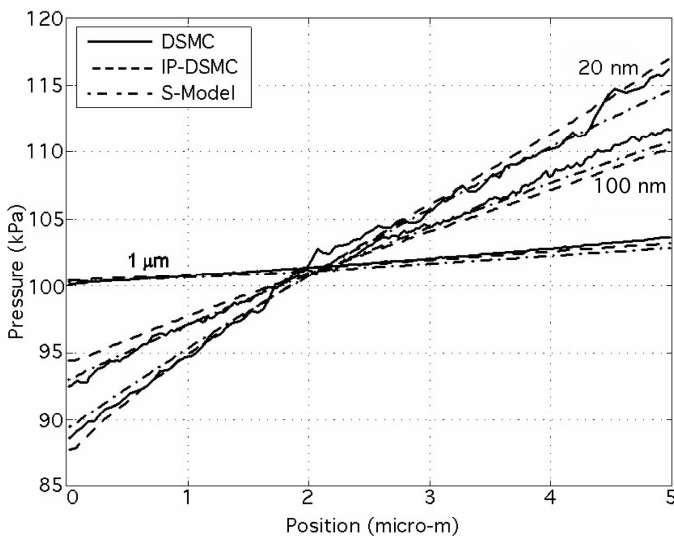


Fig. 8: Pressure profiles for various channel heights, corresponding to a test case for which the temperature profile was assumed to be linear and ΔT = 300K. The results from DSMC, IP-DSMC and from the S-model are in close agreement with each other for all three cases.

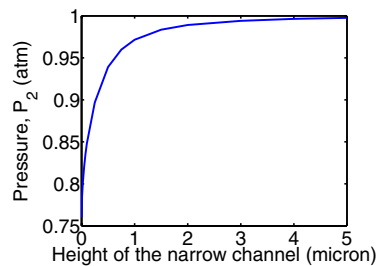


Fig. 9: With P<sub>1</sub> at atm., reducing channel height can lead to significantly improved pressure ratios. Width of channel assumed at 10 μm.

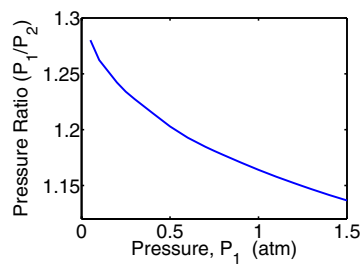


Fig. 10: Pressure ratio (P<sub>1</sub>/P<sub>2</sub>) improves for lower hot end pressures (P<sub>1</sub>). (Assumes channel height = 0.1 μm and channel width = 10 μm.)

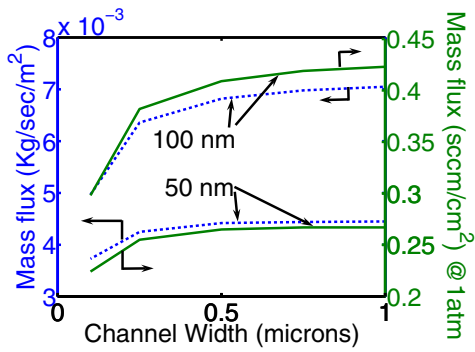


Fig. 11: Mass flux and equivalent flow at ambient pressure for 50 nm and 100 nm channel heights.

the simulation results and experimental measurements is expected to reduce as the temperature model is refined and the pressure measurement error is reduced.

Figure 8 shows the pressure profile from a series of numerical simulations that were performed on channels with a length of 5  $\mu\text{m}$ , various heights (1  $\mu\text{m}$ , 100 nm and 20 nm), and linearly varying temperature from 273 K to 573 K along the channel. The plots suggest that the results from Sharipov's model closely resemble to the DSMC and IP-DSMC results in this context; IP-DSMC being a more efficient DSMC technique [13].

Figure 9 shows the variation of the cold end pressure ( $P_2$ ) with the reduction in channel heights, as predicted by Sharipov's model, for the 700  $\mu\text{m}$  long channel. The rate of decrease of  $P_2$  increases with decreasing channel heights. This suggests that the device performance is enhanced with decreasing channel heights, potentially because the thermal transpiration effects become increasingly more pronounced for channel heights less than 100 nm.

Further, it is observed that with the reduction in hot cavity pressure ( $P_1$ ), a better vacuum can be generated (i.e. higher  $P_1/P_2$ ) (Fig. 10). This indicates that an open system, for which cavity 3 is vented to the ambient so that  $P_1$  can never exceed 1 atm., is more effective than a closed system. Moreover, it also predicts that a multistage pump will benefit from higher-pressure ratios in successive stages.

Finally, Sharipov's model was used to evaluate mass flux of gas through narrow channels with heights 50 nm (channel A) and 100 nm (channel B) at ambient pressure (Fig. 11). The analysis suggests that as the height-to-width ratio reduces from unity, the mass flux through a channel of a given height increases and then attains a saturation value for widths much larger than the height. This indicates that depending on the fabrication complexities, one can choose to have multiple channels with smaller widths, so long as the mass flux is in saturation regime.

## V. CONCLUSION

The study suggests that Sharipov's model can be used as preliminary tool to predict the behavioral response a micro system. Application of Sharipov's model to the Knudsen pump design suggests that: (a) in this particular context, the channel length can be reduced to 200  $\mu\text{m}$  without severely affecting the performance of the device. (b) Increasingly higher pressure ratio ( $P_1/P_2$ ) can be attained by lowering pressure  $P_1$  in the hot chamber, thus predicting higher pressure ratios in the successive stages of a multi-stage Knudsen pump. (c) The mass flow rate calculations using Sharipov's model indicates that the mass flux increases with the channel height (for narrow channels), and for a channel with given height, the mass flux first increases with increasing width and then attains a saturation value for widths much larger than channel height.

## REFERENCES

- [1] O. Reynolds, *Philos. Tran. Royal Society*, Ser. B, v.170, 1879, pp. 727-845
- [2] J. Maxwell, "On stresses in Rarefied Gases Arising from Inequalities of Temperature," *Philos. Tran. Royal Society*, v. 170, 1879, pp. 231-256
- [3] L. Loeb, *The Kinetic Theory of Gases*, McGraw Hill, 1934, pp. 355-359
- [4] M. Knudsen, *Ann. Phys.*, v. 31, 1910, pp. 205-229
- [5] E. Zellers, et. al., "Recent Developments in Gas Chromatographic Microsystems," *IEEE Transducers '07*.
- [6] G. Bird, *Molecular Gas Dynamics and the Direct Simulation of Gas Flows*. Oxford, UK, 1994
- [7] E. Oran, C. Oh, B. Cybyk, "Direct Simulation Monte Carlo: Recent Advances and Applications," *Annu. Rev. Fluid Mech.*, 30, 1998, pp. 403-441
- [8] S. McNamara, Y. Gianchandani, "On-Chip Vacuum Generated by a Micromachined Knudsen Pump," *JMEMS*, 14(4), 2005, pp. 741-746
- [9] E. Kennard, *Kinetic Theory of Gases*, McGraw Hill, 1938. pp. 327-332
- [10] J. Williams III, "Thermal Transpiration - A Continuum Gasdynamics View," *J. Vac. Sci. Technol.*, v.8, 1970, pp. 446-450
- [11] F. Sharipov, "Non-isothermal gas flow through rectangular microchannels," *JMM*, v.9, 1999, pp. 394-401
- [12] N. Gupta, Y. Gianchandani, "Modeling and Simulation of a Surface Micromachined Knudsen Pump," *ASME Congress*, 2006, pp. 1-7
- [13] N. Masters, "Efficient Numerical Techniques for Multiscale Modeling of Thermally Driven Gas Flows with Application to Thermal Sensing Atomic Force Microscopy," *Ph.D. Thesis, Georgia Institute Technology*, June 2006